Dynamic Wireless Power Transfer DWPT Time Domain model: *xyz* position and speed coupling effect

Iosu Aizpuru[1], Eneko Agirrezabala[1], Mikel Mazuela[1], Unai Iraola[1], Estanis Oyarbide[2], Carlos Bernal[2]
[1]Mondragon Unibertsitatea, Mondragon, Spain
[2]University of Zaragoza, Zaragoza, Spain
E-Mail: iaizpuru@mondragon.edu
URL: https://www.mondragon.edu/en/research-transfer/engineering-technology/research-transfer-group/energy-storage

Acknowledgements

This research project is financially supported by CDTI program MISIONES. The name of the project is CARDHIN. The project is also supported by Ministerio de Ciencia, Innovación y Universidades.

Keywords

« Wireless power transmission », « Electric vehicle », « Time-domain analysis », « Battery charger», « Contactless Energy Transfer»

Abstract

The paper presents a DWPT system time domain model which considers speed $(\dot{x}, \dot{y}, \dot{z})$ and position (x, y, z) coupling effects. The speed effect compared to static WPT, presents an active behavior that should be considered during the coil design stage. The model is generalized and validated for resonant WPT systems and dynamic speed influenced DWPT systems.

1. Introduction

Greenhouse Gas Emissions GHG are increasing and are the main contributors to the global warming effect, breaking new temperature records since data calculation started in 1880 [1]. 72% of the GHG emissions generated are due to the energy sector, where road transportation (light-mid-heavy vehicles) are responsible of the 11.9% of the emissions [2]. For this reason, the electric vehicle is a great asset or candidate to help in the mitigation of the GHG emissions in the XXI century [3].

For the massive insertion in society of the electric vehicle, two major challenges must be solved: improving battery technology and designing a sustainable charging infrastructure. Referring to the charging infrastructure, this infrastructure must offer a great diversity of charging methods, be sustainable and at the same time have the capacity to supply the power of electric vehicles. There are different charging methods. Some differ by charging power (slow charging - fast charging). Others differ by the charging method (wired charging, wireless etc). Wireless charging systems are mainly static systems but dynamic wireless power transfer systems DWPT [4] are emerging as a new alternative within the charging infrastructure. DWPTs **Fig. 1 a)** allow the reduction of stops for battery charging, minimize the DOD of the batteries, increasing the useful life and even allow the optimization of the size of the battery [5]. In turn, this enables the use of smaller batteries, reducing the costs and facilitating the insertion in society of the electric vehicle [6].

Although DWPT technology is incipient and novel, there are studies that try to analyze and understand the problem of wireless charging systems. DWPT systems suffer mainly from misalignments, with some studies analyzing the effect of misalignments in the longitudinal road direction (*x* axis in this article) in steady state [7]–[9]. Low number of Publications make reference to misalignments in other axis as lateral misalignment, and they are classically limited to steady state analysis [10]. Limited analysis has been

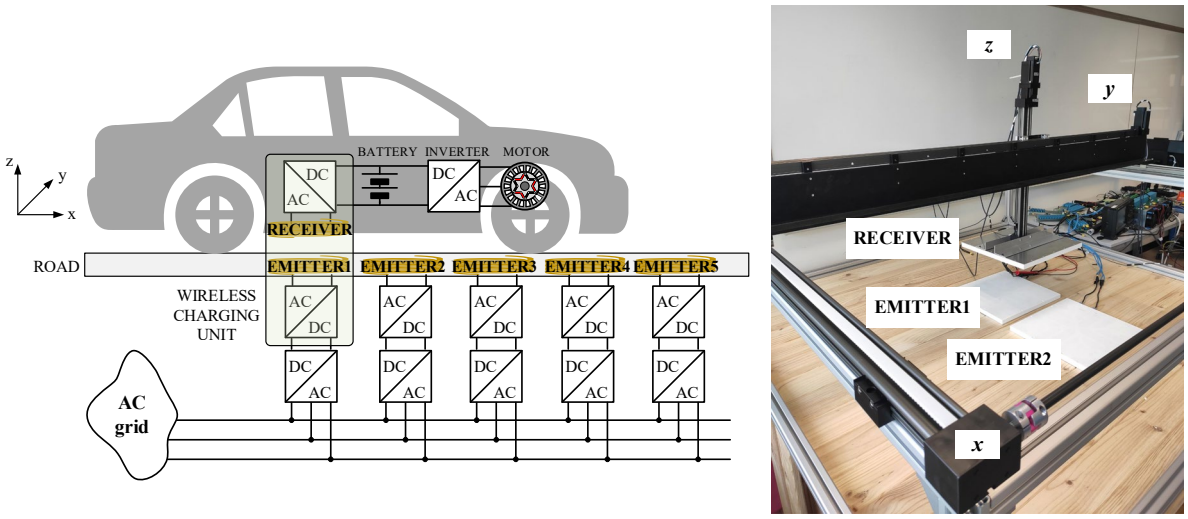

a) **b)**

Fig. 1: a) Classical Dynamic Wireless Power Transfer DWPT schematic diagram. EMITTER: The energy comes from the AC grid, rectified and transformed to the emitter coil through a high frequency wireless charging unit. RECEIVER: The receiver is the Electric Vehicle where the energy is obtained through the wireless charging unit receiver coil, inserted to the battery through a high frequency converter and after transformed to mechanical energy by a power train composed of an inverter and a motor. WIRELESS CHARGING UNIT: Wireless charging unit composed of 2 high frequency AC-DC converters in emitter and receiver coupled by 2 air coupled coils. **b)** Developed 3D experimental platform for speed $(\dot{x}, \dot{y}, \dot{z})$ and position (x, y, z) misalignments analysis in DWPT systems.

done related to the influence of speed in DWPT systems, mainly concluding that the speed is not relevant in DWPT systems [11], [12]. Different control structures have been analyzed in order to maximize the transferred energy, but they are limited to steady state analysis [11], [13]–[16].

After the analysis of DWPT state of the art it is clear that there is a lack of modelling effort regarding different topics.

- DWPT modelling is mainly focused on steady state phasor modelling and there is a lack of investigation regarding dynamic time domain models.
- DWPT is clearly influenced by misalignments. However, the state of the art presents reduced number of analysis regarding misalignment effects. Longitudinal (x), lateral (y) and vertical (z) misalignments should be taken into account.
- DWPT systems permit to charge EVs during movement. The moving effect inserts another uncertainty to the modelling issue, the coupling of this speed $(\dot{x}, \dot{y}, \dot{z})$ in the DWPT system. This coupling is not deeply analyzed in the state of the art.

The contributions of this research paper will try to mitigate the lack of investigation in DWPT modelling, by developing a dynamic time domain model for DWPT systems where longitudinal (x, $\dot{x}$), lateral (y, $\dot{y}$) and vertical (z, $\dot{z}$) position and speed coupling are considered.

The research paper starts with an introduction regarding the state art and the main contributions of the research paper. Section 2 presents the basics regarding wireless power transfer systems modelling. Section 3 develops the 3-axis speed and position coupled model. Section 4 analyses how to augment the model order to implement a static resonant WPT system. Section 5 validates the model under a dynamic behavior analyzing the model sensitivity to speed variations. Finally, the main conclusions of the paper are presented.

2. Wireless charging basics modelling

Wireless charging units are composed by two power converters working in the emitter (infrastructure side) and the receiver (EV side) and a wireless coupling system composed of coils. The power converters

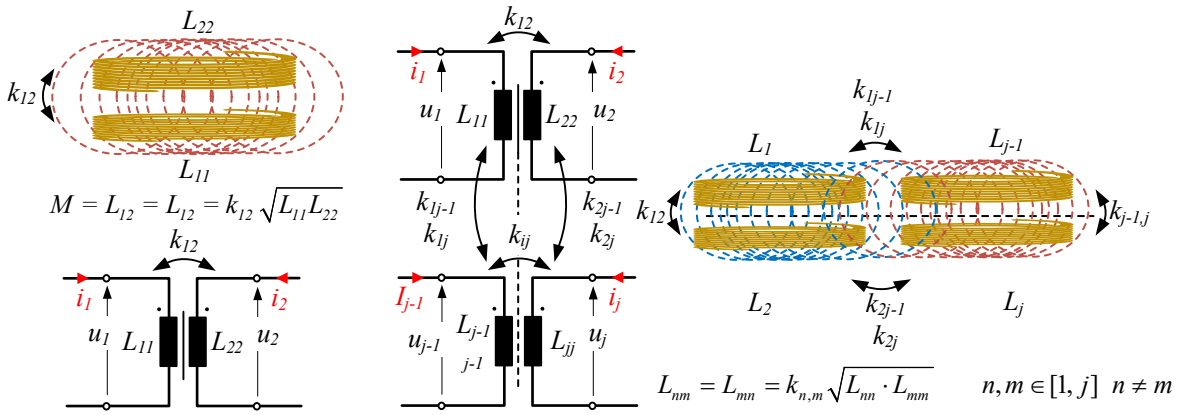

a) **b)**

Fig. 2: Wireless power Transfer coil modelling. Model for 2 coupling coils represented by **a)** and **b)** generalized model for *j* coupled coils, where coils could be part of the transmitter or receiver circuit.

could be represented as 2 voltage sources for the sake of simplicity. The coupling between the emitter and the receiver is developed by 2 coils. Instead of a high coupling magnetic core, due to the inherit need of Wireless Power Transfer systems, the coupling media of these 2 coils is air.

The basic WPT system is modelled by the 2 auto inductances $\boldsymbol{L_{11}}$ and $\boldsymbol{L_{22}}$ of the emitter and transmitter coils, and the coupling inductor $\boldsymbol{L_{12} = L_{21}}$ which models the coupling flux between both coils **Fig. 2 a)**. This coupling inductance is related with the auto inductances by the coupling factor $\boldsymbol{k}$ which could be identified as $\boldsymbol{k_{12}}$ for the basic coupling between 2 coils. The voltage induced in each coil $\boldsymbol{u}$ is directly the time derivative of the flux linkage $\boldsymbol{\Psi}$ of each of the coils. This magnetic analysis can be written by equations (1) and (2) and wrapped in a matrixial way by (3).

$$M = L_{12} = L_{21} = k_{12}\sqrt{L_{11} \cdot L_{22}} = k\sqrt{L_{11} \cdot L_{22}} \qquad (1)$$

$$u_1 = \frac{\partial \Psi_1}{\partial t} = L_{11}\frac{\partial i_1}{\partial t} + M\frac{\partial i_2}{\partial t} \;\; ; \;\; u_2 = \frac{\partial \Psi_2}{\partial t} = L_{22}\frac{\partial i_2}{\partial t} + M\frac{\partial i_1}{\partial t} \qquad (2)$$

$$\begin{bmatrix} u_1 \\ u_2 \end{bmatrix} = \begin{bmatrix} \frac{\partial \Psi_1}{\partial t} \\ \frac{\partial \Psi_2}{\partial t} \end{bmatrix} = \begin{bmatrix} L_{11} & L_{12} \\ L_{21} & L_{22} \end{bmatrix} \cdot \begin{bmatrix} \frac{\partial i_1}{\partial t} \\ \frac{\partial i_2}{\partial t} \end{bmatrix} \qquad (3)$$

The problem analyzed for 2 coils WPT could be generalized to $\boldsymbol{j}$ number of coils as presented in **Fig. 2 b)**. The generalized form composed by $\boldsymbol{j}$ coils could implement different configurations (1 receiver, j-1 transmitters; j-1 receivers, 1 transmitter, etc.) which leads to a general model that could model any DWPT or WPT configuration. The general model presented in **Fig. 2 b)** could be expressed by equations (4) and (5) for any coil $\boldsymbol{n,m}$ which belongs to the $\boldsymbol{j}$ coils. Equations (4) and (5) could be merged in (6). The voltage of each inductor could be merged by equation (7) where the auto inductances and mutual inductances are represented by the general inductance $\boldsymbol{L_{nm}}$.

$$L_{nm} = L_{mn} = k_{n,m}\sqrt{L_{nn} \cdot L_{mm}} \qquad n, m \in [1, j] \;\; n \neq m \qquad (4)$$

$$u_n = \frac{\partial \Psi_n}{\partial t} = L_{nn}\frac{\partial i_n}{\partial t} + \ldots + \sum_{\substack{m=1 \\ n \neq m}}^{j} L_{nm}\frac{\partial i_m}{\partial t} \;\; ; \;\; u_m = \frac{\partial \Psi_m}{\partial t} = L_{mm}\frac{\partial i_m}{\partial t} + \ldots + \sum_{\substack{m=n \\ n \neq m}}^{j} L_{mn}\frac{\partial i_n}{\partial t} \qquad (5)$$

$$\begin{bmatrix} u_1 \\ \vdots \\ u_j \end{bmatrix} = \begin{bmatrix} \frac{\partial \Psi_1}{\partial t} \\ \vdots \\ \frac{\partial \Psi_j}{\partial t} \end{bmatrix} = \begin{bmatrix} L_{11} & \cdots & L_{1j} \\ \vdots & \ddots & \vdots \\ L_{j1} & \cdots & L_{jj} \end{bmatrix} \cdot \begin{bmatrix} \frac{\partial i_1}{\partial t} \\ \vdots \\ \frac{\partial i_j}{\partial t} \end{bmatrix} \quad (6)$$

$$u_n = \frac{\partial \Psi_n}{\partial t} = \sum_{m=1}^{j} L_{nm} \frac{\partial i_m}{\partial t} \quad (7)$$

However, this generalized model does not include the dynamic (speed $(\dot{x}, \dot{y}, \dot{z})$ and position (x, y, z) misalignments) effects of DPWT systems, so this model should be modified in order to undercome DPWT system modelling and simulations.

3. DWPT modelling: *(x,y,z)* speed and position coupling

Compared to the general static model presented in Section 2 which represents constant values for the auto inductance and mutual inductances of different transmission coils, a DWPT system has variable parameter values that could be modelled due to the changing value of the coupling factor ***k.***

According to equation (7) any ***n*** inductor could be defined by the sum of all the coupling voltages. However in a DPWT system the inductance value is variable as a function of the position (x, y, z) as defined by equation (8).

$$L_{nm}(t) = f_{nm}(x(t), y(t), z(t)) \quad (8)$$

Equations (2),(5) and (7) are a simplified version of the derivative of flux due to the assumption of constant inductors in static WPT systems; as it is presented in equation (9). However, DWPT systems do not have constant inductance values as presented in equation (8), so the derivative of flux is expressed by equation (10).

$$u_n = \frac{\partial \Psi_n}{\partial t} = \sum_{m=1}^{j} \frac{\partial \{L_{nm} \cdot i_m(t)\}}{\partial t} = \sum_{m=1}^{j} L_{nm} \frac{\partial i_m}{\partial t} \text{ ; static WPT equation (7)} \quad (9)$$

$$u_n = \frac{\partial \Psi_n}{\partial t} = \sum_{m=1}^{j} \frac{\partial \{L_{nm}(t) \cdot i_m(t)\}}{\partial t} = \sum_{\substack{p=x,y,z \\ m=1}}^{j} \frac{\partial L_{nm}}{\partial p} \frac{\partial p}{\partial t} i_m(t) + \sum_{m=1}^{j} L_{nm}(t) \frac{\partial i_m(t)}{\partial t} \text{ ; dynamic DWPT} \quad (10)$$

The general DWPT expression presented in equation (10) presents a speed term ***δp/δt***. If this speed term is expanded as ***δp/δt*** = $(\dot{x}, \dot{y}, \dot{z})$ equation (10) could be expressed as equation (11).

$$u_n = \frac{\partial \Psi_n}{\partial t} = \underbrace{\sum_{m=1}^{j} \left(\frac{\partial L_{nm}}{\partial x} \dot{x} + \frac{\partial L_{nm}}{\partial y} \dot{y} + \frac{\partial L_{nm}}{\partial z} \dot{z} \right) i_m(t)}_{ACTIVE\ BEHAVIOUR} + \underbrace{\sum_{m=1}^{j} L_{nm}(t) \frac{\partial i_m(t)}{\partial t}}_{REACTIVE\ BEHAVIOUR} \quad (11)$$

Equation (11) presents the main difference of a DWPT system vs a static WPT: The influence of speed to the system. Analyzing equation (11) 2 different components could be analyzed:

- REACTIVE BEHAVIOUR ($v_L = L \cdot di/dt$): Same behavior as in a static WPT system presented in equation (7) but with variable and position dependent inductances ***$L_{nm}(t)$*** defined in (8).
- ACTIVE BEHAVIOUR ($v = R \cdot i$): The voltage induced in the inductor is influenced by a speed dependent parameter multiplied by the current flowing in the inductor, modelled by an active behavior.

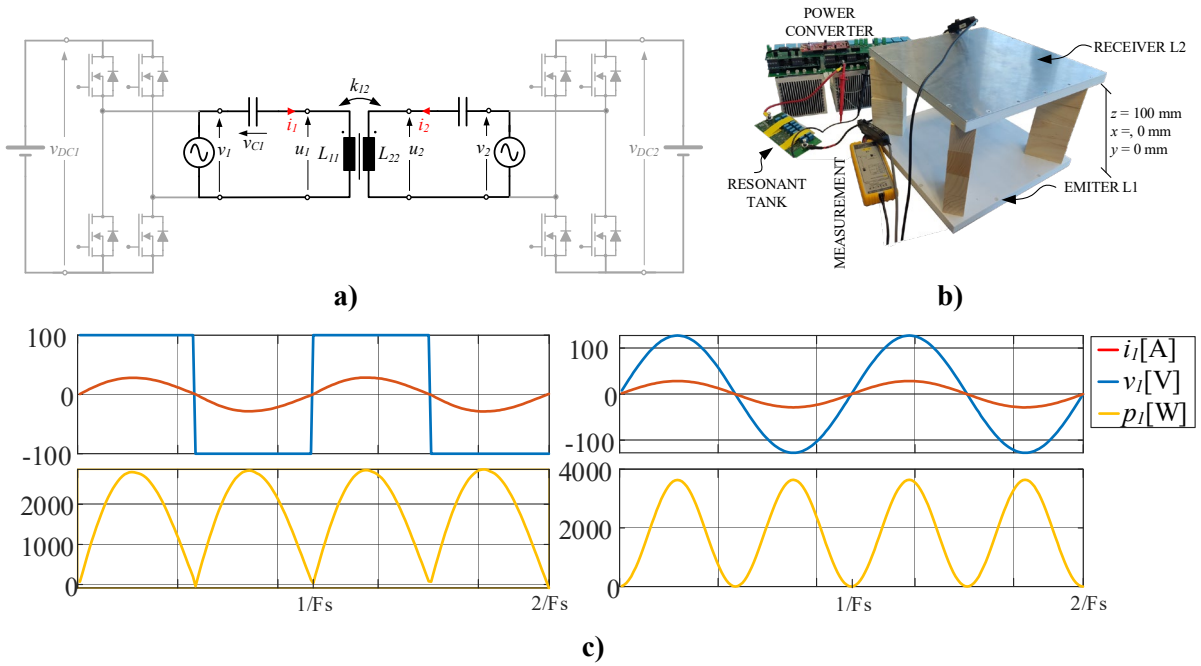

Fig. 3: Analysis of a series compensated resonant system. **a)** Modelled circuit with equivalent phasor/sinusoidal voltage generation or real converter operation. **b)** Developed experimental WPT system for model validation with 350 mm x 350 mm square WPT coils. **c)** Model results WPT resonant converter: LEFT: Real converter square excitation RIGHT: Phasor/Sinusoidal excitation. Results for primary side instantaneous voltage, current and power (i_1,v_1,p_1).

So as a conclusion, for modelling a DWPT system is mandatory to obtain the variable magnetic coupling components $\boldsymbol{L_{nm}(t)}$ and the model will suffer some active behavior due to the speed of the DWPT system.

4. Model Use Case 1: Augmented static model for resonant coupling.

Models developed in Section 2 and 3 are representative for static and dynamic wireless transfer systems. The developed models only focus on the magnetic coupling between the different coils of a wireless power transfer system. However, wireless power transfer systems need a compensation network in order to maximize the transferred energy between the emitter and the receiver coils. This compensation networks are resonant networks that are tuned in order to maximize the coupling effect of the WPT coils. The model presented in Section 2 and 3 should be easily augmented to a resonant circuit in order to represent a real WPT system with the compensation resonant network.

Fig. 3 represents a classical series compensated resonant WPT system architecture. In order to increase the model order to a series resonant configuration, input voltages v_1,v_2 and resonant capacitor voltages v_{C1},v_{C2} should be inserted to the model.
Input voltages v_1 and v_2 could be modelled by the simplified sinusoidal approach used in resonant converters or could be modelled by the square wave generated by a classical front-end full bridge converter.
Converter voltages v_1 and v_2 could be defined by equations (12) and (13) depending on the adopted modelling option (sinusoidal approach or square wave approach)

$$v_1 = \frac{4 \cdot V_{DC1}}{\pi}\sin(\omega t + \varphi_1); \quad v_2 = \frac{4 \cdot V_{DC2}}{\pi}\sin(\omega t + \varphi_2)\ ; \text{Sinusoidal fundamental approach} \qquad (12)$$

$$v_1 = V_{DC1} \cdot \text{square}(t, \varphi_1); \quad v_2 = V_{DC2} \cdot \text{square}(t, \varphi_2); \text{Power converter square wave approach} \qquad (13)$$

The square function (square(t,φ)) represents the power converter modulation technique. φ_1 *and* φ_2 represent the phase shift difference between the voltage introduced to the WPT system and is classically used to control the power transferred between V_{DC1} and V_{DC2}.

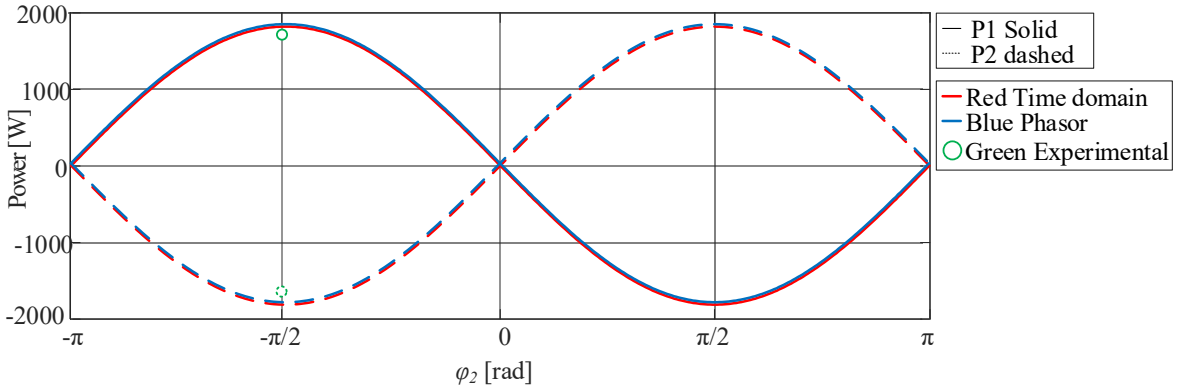

a)

Fig. 4: Simulation results of the developed validation environment presented in **Fig. 3** and parametrized in **Table I**. Compared variables: average power $\left(P = \frac{1}{T}\int_0^T p(t)dt\right)$ P1(solid) and P2 (dashed), in the proposed time domain model (red), steady state phasor model (blue) and experimental platform (green circles)

The voltage u_1 and u_2 in the coupling WPT system is defined by equations.

$$u_1 = v_1 - v_{C1}; \quad u_2 = v_2 - v_{C2}; \tag{14}$$

$$i_1 = i_{C1} = C_1 \frac{dv_{C1}}{dt}; \quad i_2 = i_{C2} = C_2 \frac{dv_{C2}}{dt}; \tag{15}$$

The combination of equations (14) and (15) with equation (3) permits to model the dynamic time domain behavior of a series resonant WPT system.

In order to validate the time-domain modelling approach, the time domain model is compared to a classical phasor steady state model and an experimental platform. The modelled system is described in **Table I**.

Table I: Parameter and variable definition for the simulation analysis of a series resonant WPT system.

Common parameters		**Primary parameters / variables**					**Secondary parameters / variables**				
$\omega = 2\pi f$	k	C_1	L_{11}	φ_1	v_1	V_{DC1}	C_2	L_{22}	φ_2	v_2	V_{DC2}
2π85kHz	0.22	94 nF	38 µH	0	sinusoidal	100 V	94 nF	38 µH	-π...π	sinusoidal	100 V

Regarding **Table I** parameters, L_{11} and L_{22} self inductances presented in **Fig. 3 b)** are experimentally measured by a LCR equipment. C_1 and C_2 are calculated to be in full resonance with the self inductances L_{11} and L_{22} at 85 kHz working frequency. The coupling factor k is experimentally measured for a constant z distance of 100 mm.

The obtained results are presented in **Fig. 4** for a secondary phase variation φ_2 from -π to π. The compared parameters are the active power of the input ports P1 and P2. The active power is calculated from the time-domain simulation as the average of the instantaneous power during a whole period. The active power from the phasor analysis is the real part of the apparent power which is defined by the multiplication between the voltage and the conjugate of the current. The active power of the experimental platform is calculated for a single φ_2 value equal to -π/2 in order to check the maximum power transfer point.
The presented results validate the developed WPT series resonant time-domain model. The results are nearly identical to the steady state phasor model. The experimental results have similar values that the simulation results. The experimental power is slightly lower due to losses in the power converter and circuit parasitic resistance.

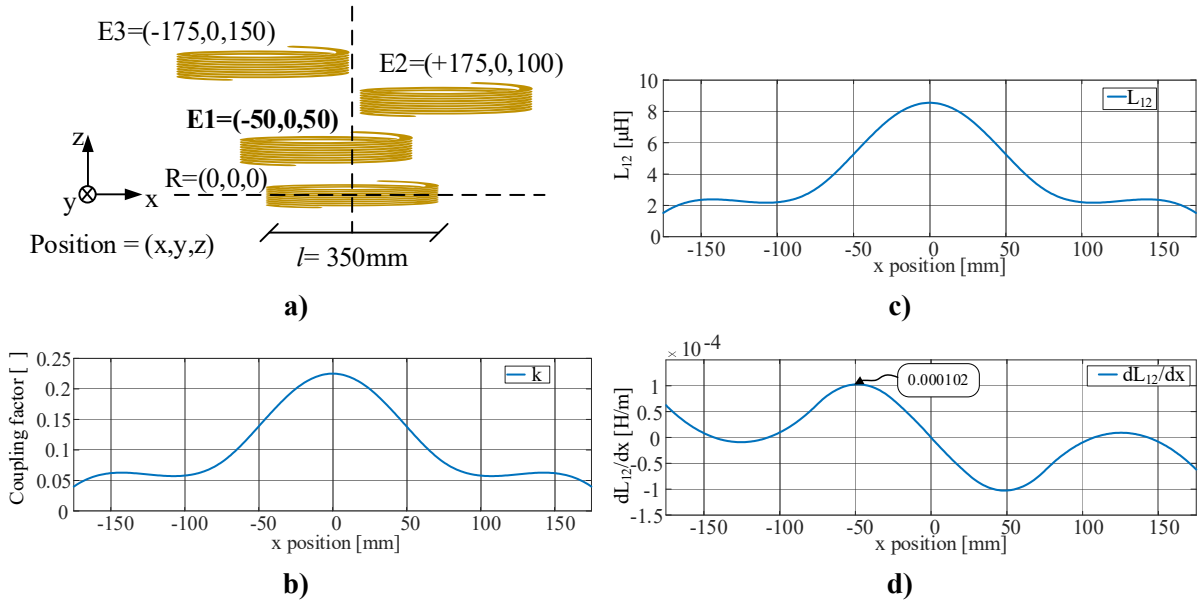

Fig. 5: Simulated DWPT system. **a)** Example of coil alignment and position reference definition in a DWPT system. **b)** Coupling factor ***k*** as a function of longitudinal misalignment *x*. **c)** Mutual inductance L_{12} as function of longitudinal misalignment x. **d)** Derivative of the mutual inductance respect to longitudinal position with a maximum value in *x*= -50mm of 0.102 µH/mm

5. Model Use Case 2: Speed influence in power loses.

The DWPT model proposed in Section 3 will be parametrized in order to analyze the speed influence in the "active behaviour" component presented in equation (11). The speed influenced model will be analyzed for the coupling effect between 2 single coils (Emitter E and Receiver R) in the longitudinal position *x* = -50mm **E1 Fig. 5 a)**, where the change in the mutual inductance due to the position is high. In order to simplify the problem, only the longitudinal speed ($\dot{x}$) effect will be analyzed. The misalignment in the lateral position *y* and height *z* will be kept constant. The auto inductance of the receiver and the emitter L_{11} and L_{22} will be assumed as constant. This assumption is valid for high *z* distances, where the self inductance of the receiver is not affected by the emitter and vice versa. Thus, only the mutual inductance $M(x,t) = L_{21}(x,t) = L_{12}(x,t)$ will vary in function of longitudinal position *x*. In order to obtain the active behavior of the speed influenced model presented in (11), the derivative of the mutual inductance with respect to the longitudinal position *x*. $\left(\delta L_{12}/\delta x\right)$ is required.

First, the mutual inductance variation effect between 2 DWPT coils is defined. The $L_{21}(x,t)$ inductance variation is totally dependent on the geometry, type and construction of the DWPT coils. The maximum coupling factor ***k*** is defined as 0.22 and is obtained when the longitudinal position is equal to 0 mm **Fig. 5 b)**. The mutual inductance is plotted for a ± 175 mm deviation which is represented in **Fig. 5 c)** for a defined coil of 350 mm total length.

After defining $L_{21}(x,t)$ the derivative $\delta L_{12}/\delta x$ is obtained. The derivative will be analyzed in *x* =-50 mm, where the influence is maximum. As presented in **Fig. 5 d)** the $\delta L_{12}/\delta x$ value for *x*= -50 mm is 0.102 µH/mm. (0.000102 H/m).

The $\delta L_{12}/\delta x$ value 0.102 µH/mm for *x*= -50 mm will be analyzed in order to check the voltage drop derived from the active behavior analyzed in equation (11). The analysis will be performed for RMS currents from 0 to 150 A (Ranges in the order of 0 to 50 kW DWPT systems) and a speed range in the longitudinal axis *x* from 0 km/h to 120 km/h.

The results presented in **Fig. 6** show that voltage drops of 0,5 V and power losses of 80 W are possible in DWPT system. These drop/losses could also increase depending on the coil geometry/sizing and if $(\dot{y}, \dot{z})$ misalignments are considered, so should be analyzed during the design process.

The developed model will be validated in future research works by the 3D experimental platform presented in **Fig. 1 b)** where speed $(\dot{x}, \dot{y}, \dot{z})$ and position (x, y, z) misalignments will be analyzed.

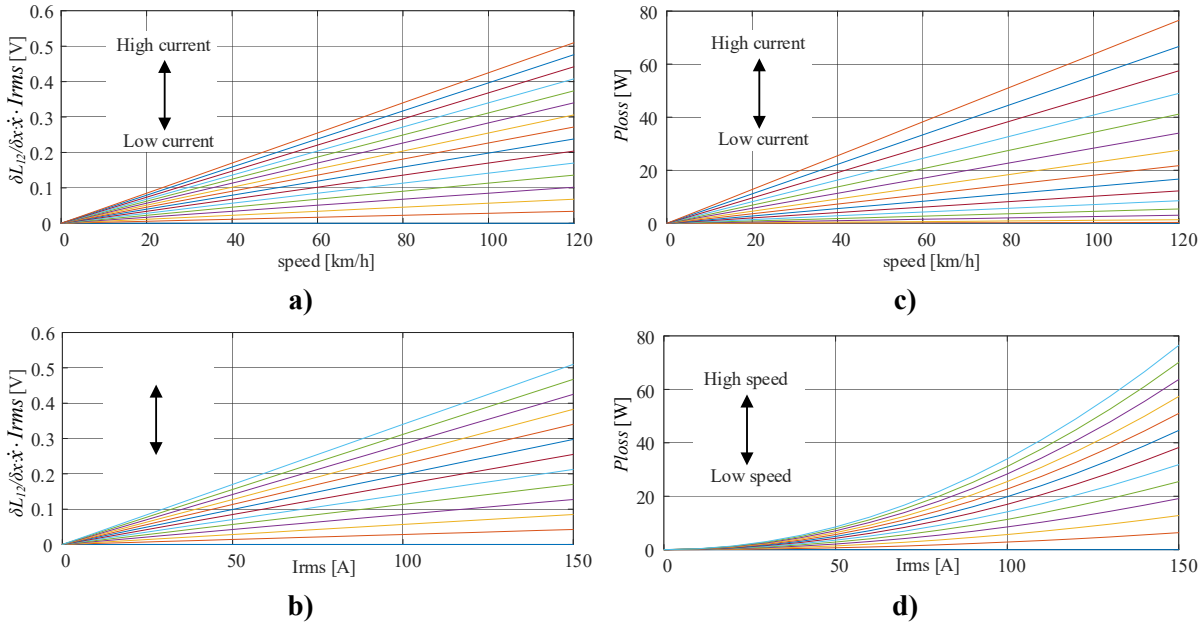

Fig. 6: Parametric analysis of primary RMS current Irms and speed $\dot{x}$ influence (Irms =0…150A, $\dot{x}$ = 0…120 km/h) .**a)** Voltage drop as a function of speed for different Irms. **b)** Voltage drop as a function of Irms for different speed. **c)** *Ploss* as a function of speed for different Irms. **d)** *Ploss* as a function of Irms for different speed

Conclusions

The develop research work presents a full Dynamic Wireless Power Transfer DWPT time-domain model that simulates the behavior of any generalized DWPT system. The developed model considers misalignments and coupling effects in the space/position domain (x, y, z) and speed $(\dot{x}, \dot{y}, \dot{z})$ domain. It is clearly presented that in DWPT systems there is a classical REACTIVE BEHAVIOR of magnetic coupling systems, but there is also an ACTIVE BEHAVIOR due to the influence of speed that should be considered.

The developed time domain model is easily augmented to reproduce a classical series resonant WPT system. The time-domain model presents same average power results as a classical phasor steady state model, and it is also validated by an experimental platform with 350mm x 350mm square WPT coils.

In order to analyze the DWPT ACTIVE BEHAVIOR under speed and current variations, the model is parametrized for a varying coupling factor $\boldsymbol{k}$ in function of the position x. The model presents a maximum voltage drop of 0.5V and power losses of 80 W for a 120 km/h and 150 A RMS values. The voltage drop and the power loss is directly dependent on the coupling factor shape and the derivative with respect to position, so it should be taken into account in the manufacturing process of DWPT coils.

The developed model will be fully validated under (x, y, z) - $(\dot{x}, \dot{y}, \dot{z})$ variations in future research works. A 3D experimental platform presented in **Fig. 1 b)** will be used in order to validate the developed time domain model.

References

[1] NOAA National Centers for Environmental Information, “State of the Climate: Global Climate Report for Annual 2019,” 2019. [Online]. Available: https://www.ncdc.noaa.gov/sotc/global/201913.

[2] World resources Institute, “Climate analysis indicators tool,” 2017, [Online]. Available:

https://www.wri.org/blog/2020/02/greenhouse-gas-emissions-by-country-sector.

[3] G. Hill, O. Heidrich, F. Creutzig, and P. Blythe, “The role of electric vehicles in near-term mitigation pathways and achieving the UK ’ s carbon budget,” *Appl. Energy*, vol. 251, no. July 2018, p. 113111, 2019, doi: 10.1016/j.apenergy.2019.04.107.

[4] R. Zeng, V. P. Galigekere, O. C. Onar, and B. Ozpineci, “Grid Integration and Impact Analysis of High-Power Dynamic Wireless Charging System in Distribution Network,” *IEEE Access*, vol. 9, pp. 6746–6755, 2021, doi: 10.1109/ACCESS.2021.3049186.

[5] X. Mou, Y. Zhang, J. Jiang, and H. Sun, “Achieving Low Carbon Emission for Dynamically Charging Electric Vehicles through Renewable Energy Integration,” *IEEE Access*, vol. 7, pp. 118876–118888, 2019, doi: 10.1109/ACCESS.2019.2936935.

[6] S. Jeong, Y. J. Jang, and D. Kum, “Economic Analysis of the Dynamic Charging Electric Vehicle,” *IEEE Trans. Power Electron.*, vol. 30, no. 11, pp. 6368–6377, 2015, doi: 10.1109/TPEL.2015.2424712.

[7] F. Lu, H. Zhang, H. Hofmann, and C. C. Mi, “A Dynamic Charging System with Reduced Output Power Pulsation for Electric Vehicles,” *IEEE Trans. Ind. Electron.*, vol. 63, no. 10, pp. 6580–6590, 2016, doi: 10.1109/TIE.2016.2563380.

[8] N. Teerakawanich, “Dynamic Modeling of Wireless Power Transfer Systems with a Moving Coil Receiver,” *ITEC Asia-Pacific 2018 - 2018 IEEE Transp. Electrif. Conf. Expo, Asia-Pacific E-Mobility A Journey from Now Beyond*, pp. 1–5, 2018, doi: 10.1109/ITEC-AP.2018.8433269.

[9] A. Rakhymbay, A. Khamitov, M. Bagheri, B. Alimkhanuly, M. Lu, and T. Phung, “Precise analysis on mutual inductance variation in dynamic wireless charging of electric vehicle,” *Energies*, vol. 11, no. 3, 2018, doi: 10.3390/en11030624.

[10] R. Tavakoli and Z. Pantic, “Analysis, Design, and Demonstration of a 25-kW Dynamic Wireless Charging System for Roadway Electric Vehicles,” *IEEE J. Emerg. Sel. Top. Power Electron.*, vol. 6, no. 3, pp. 1379–1393, 2018, doi: 10.1109/JESTPE.2017.2761763.

[11] T. Fujita, T. Yasuda, and H. Akagi, “A Dynamic Wireless Power Transfer System Applicable to a Stationary System,” *IEEE Trans. Ind. Appl.*, vol. 53, no. 4, pp. 3748–3757, 2017, doi: 10.1109/TIA.2017.2680400.

[12] Y. Guo, L. Wang, Q. Zhu, C. Liao, and F. Li, “Switch-On Modeling and Analysis of Dynamic Wireless Charging System Used for Electric Vehicles,” *IEEE Trans. Ind. Electron.*, vol. 63, no. 10, pp. 6568–6579, 2016, doi: 10.1109/TIE.2016.2557302.

[13] A. Babaki, S. Vaez-Zadeh, and A. Zakerian, “Performance Optimization of Dynamic Wireless EV Charger under Varying Driving Conditions without Resonant Information,” *IEEE Trans. Veh. Technol.*, vol. 68, no. 11, pp. 10429–10438, 2019, doi: 10.1109/TVT.2019.2944153.

[14] Z. Zhou, L. Zhang, Z. Liu, Q. Chen, R. Long, and H. Su, “Model Predictive Control for the Receiving-Side DC-DC Converter of Dynamic Wireless Power Transfer,” *IEEE Trans. Power Electron.*, vol. 35, no. 9, pp. 8985–8997, 2020, doi: 10.1109/TPEL.2020.2969996.

[15] F. Liu, Y. Yang, Z. DIng, X. Chen, and R. M. Kennel, “A Multifrequency Superposition Methodology to Achieve High Efficiency and Targeted Power Distribution for a Multiload MCR WPT System,” *IEEE Trans. Power Electron.*, vol. 33, no. 10, pp. 9005–9016, 2018, doi: 10.1109/TPEL.2017.2784566.

[16] H. He *et al.*, “Maximum Efficiency Tracking for Dynamic WPT System Based on Optimal Input Voltage Matching,” *IEEE Access*, vol. 8, pp. 215224–215234, 2020, doi: 10.1109/ACCESS.2020.3041769.